Surface characteristics of titanium based coatings obtained by detonation spraying under various process conditions

Vyacheslav V. Sirota[1], Sergey E. Savotchenko[2,3*], Valeriya V. Strokova[1], Daniil S. Podgornyi[1], Sergey V. Zaitsev[1], Anton S. Churikov[1], Marina G. Kovaleva[4]

[1] Belgorod V. G. Shoukhov State Technological University, 46 Kostyukova str., Belgorod, 308012, Russia

[2] Russian Sergo Ordzhonikidze State Geological Prospecting University Miklukho-Maklaya St., 23, 117997, Moscow

[3]Moscow Technical University of Communications and Informatics, Aviamotornaya St., 8a, 111024, Moscow, Russia

[4]Belgorod State National Research University, 85 Pobedy str., Belgorod, 308015, Russia

[*]Corresponding author: savotchenkose@mail.ru

Abstract.

The surface properties of metal-ceramic coatings based on titanium dioxide are described in dependence on the detonation spraying conditions. It is found that such properties as surface roughness, surface thickness, and their hydrophobicity can be controlled in the production process by selecting certain values of the technological parameters of the spraying process. The optimal values of the technological parameters of detonation spraying, ensuring maximum hydrophobicity of the produced coatings, are determined. The roughness of the coating surface and the coating thickness depend on the speed of the nozzle passage in accordance with the inverse power law. The roughness and the contact angle depend on spray distance in accordance with a parabolic law. New equations are obtained that can be useful for predicting the characteristics of the coating surface, as well as for determining the optimal mode of spraying the coating, ensuring its best hydrophobicity.

Keywords: ceramics coatings; titanium dioxide coatings; detonation spraying; contact angle; roughness; surface characteristics; spray distance; speed of nozzle passage; titanium dioxide;

1. Introduction

The application of protective metal-ceramic coatings can improve the performance properties and durability of structural materials [1, 2]. Development and modification of

[DOI: 10.22068/ijmse.4073]

coating surfaces is widely used in various fields [3, 4]. However, the required properties of coatings can be obtained at the stage of their production by optimizing the technological application process [5, 6].

Research in the field of developing new methods for improving the surface of titanium-based coatings has remained relevant for a number of years [7, 8, 9]. At the same time, methods for applying metal-ceramic coatings are being actively developed and improved [10, 11, 12]. The detonation spraying method should be highlighted as particularly promising [13, 14, 15]. Titanium coatings are often applied in this manner [16-19].

Metal-ceramic composite coatings have photocatalytic properties and therefore are widely used [20, 21], including as self-cleaning protective coatings [22, 23] and materials for biotechnology [24, 25]. It should be noted that studies were conducted on the influence of various technological parameters of detonation spraying on the properties of titanium coatings [26, 27, 28].

Recently we reported on the development of composite metal-ceramic coatings by detonation spraying and described their structure and photocatalytic properties [29]. The influence of the value of energy density flux on the rate constant of the photocatalytic reaction of TiO_2 coatings obtained by detonation spraying was studied in [30]. To predict the values of the rate constant of the photocatalytic reaction depending on the density of ultraviolet radiation, the theoretical models were formulated. It was found that the parabolic equation could be used to fit the experimental data. The phenomenological model based on a differential equation was proposed, and its solution was obtained. It was shown that the obtained solution sufficiently describes dependence of the photocatalytic rate constant on the energy flux density.

The influence of the regimes of detonation spraying the Ti-TiO_2-based coatings on its photocatalytic properties was studied in [31]. It was found that the photocatalytic activity and the rate constant of the photocatalytic reaction of the coatings decrease with an increase in the spray distance. Results showed that the photocatalytic activity and the rate constant of the photocatalytic reaction of coatings increase with an increase in the rutile percentage. Two new equations were proposed. The first one describes the decreasing of the photocatalytic rate constant according to a power law with an increase in the spray distance. The second one describes the increasing of the photocatalytic activity according to an exponential law with an increase in the rutile percentage.

In the present paper, we research the effect of detonation spraying process conditions on the surface characteristics of the metal-ceramic dioxide titanium coatings. The importance of studying the influence of technical parameters that can be controlled in the process of

[DOI: 10.22068/ijmse.4073]

detonation spraying on the properties of the coating surface has been noted by many authors [32, 33]. We were able to establish new patterns of change in the surface properties of coatings sprayed using the detonation method under different operating modes of the spraying equipment.

2. Materials and Methods

The titanium powder of PTS-1 grade (JSC Polema, Russia, selected fraction of 40-60 μm) is applied at the steel samples 40x40 mm of St3 grade (National Standard 380-2005, Russia, corresponding to the steel A57036 grade, ASTM/ASME, USA) by detonation spraying, the surface of which was preliminary degreased and sandblasted.

The coatings were manufactured using a robotic complex (IntelMashin LLC, Moscow, Russia) [34, 35, 36] under various process conditions. The basic process characteristics are as follows: the barrel length is 300 mm, the barrel diameter is 18 mm, the powder feed rate is 300, g/h. Flow rates of fuel mixture components are following: air - 1.3/1.54, m^3/h, oxygen - 2.44/3.04, m^3/h, propane - 0.56/0.67, m^3/h, (cylindrical/ring form combustion chamber). The varying process characteristics are following: the spray distance - 40-80, mm; the speed of nozzle passage 400 to 2000, mm/min.

Measurements of the surface characteristics of the coatings were carried out at room temperature for samples obtained with combinations of each of the specified values of the spraying parameters. The thickness of the coatings was measured using a magnetic thickness gauge MT-201-00 (range of measured values 5-2100 μm; permissible absolute error limit ± (0.03X+1)). The measurement was carried out in accordance with ISO 2808. Each measurement was repeated 5 times, and the average value was taken as the result.

The surface roughness of the coatings was measured in the visible field of a direct optical metallographic microscope MT-24RF (SIAMS, China) using the SIAMS 800 software package (SIAMS, Russia). This software package has the function of constructing a relief along intersecting focal planes. The contact angle was measured by a KRUSS DSA30E distilled water droplet shape analyzer (KRUSS, Germany). Distilled water with a droplet volume of 4 μl and a stabilization waiting time of 30 s was used as a liquid.

To determine the roughness of the obtained 3D coating surface using the focus-variable optical method (ISO-25178-606-2015) on 3x3 mm sections, 5 sections were examined for each sample (4 corner sections at a distance of ≈5 mm from the corner and 1 central section). The roughness was determined using a grid consisting of at least 15 lines for each studied area, which ensures high internal statistical stability of each individual measurement.

[DOI: 10.22068/ijmse.4073]

Similarly, wetting angles were calculated as the average value of at least 5 droplets applied in different areas of the same coating.

3. Results and discussion

Experimental data of the thickness of coatings, roughness of their surfaces and contact angle measurements are presented in Tables 1, and 2.

All measured characteristics one can consider as the functions of two variables of the spraying regimes, such as the speed of nozzle passage s and the spray distance d: the roughness of the coating surfaces $Ra=Ra(s, d)$, the coating thickness $h=h(s, d)$, the contact angle $\theta=\theta(s, d)$.

3.1 Roughness

Fig. 1 visualizes 3D images of a section of the coating surfaces with a visible field of 3000x2000 microns. It is a graphical representation of the coating surface, which was used to determine the roughness and profile. Fig. 1 (*a*) shows the maximum value along the Z axis of 421.92 μm, and Fig. 1 (b) shows the maximum value of 251 μm. It is also visually evident that the surface irregularities are more pronounced in Fig. 1 (*a*). A typical surface for all samples is a bumpy surface with hemispherical bumps, which is due to the shape of the original powder. The size of each individual bump is also comparable to the size of an individual ball (20-40 μm). Fig. 1 (*a*) shows a coating with a lower nozzle speed, which causes the presence of large bumps measuring 200-1000 μm and a height exceeding the periodic structure by 100-300 μm (non-periodic structure). Such structures appear as a result of the fusion of powder particles due to greater heating of the powder from the detonation flow jet. In this case, the coating in Fig. 1 (*b*) has a uniformly rough periodic structure, which is due to the lower energy transferred to the substrate from the detonation gun.

The roughness *Ra* of surfaces of all coatings obtained using all 25 detonation spraying regimes used by us is varied in the range from 12.1 to 33.6 μm (see Table 2). The average roughness *Ra* of all coatings is 19.96±2.59 μm. The roughness *Rz* of surfaces of all coatings is varied in the range from 69.8 to 169.6 μm. The average roughness *Rz* of all coatings is 110.44±10.77 μm. The roughness *Rmax* of surfaces of all coatings is varied in the range from 68.9 to 159.8 μm. The average roughness *Rmax* of all coatings is 105.80±10.17 μm. The values of the roughness characteristics *Rz* and *Rmax* differ slightly.

Selecting a higher nozzle speed produces samples with a smoother coating surface at all spray distances (see Fig. 2). Therefore, one can say that the roughness *Ra* monotonically reduces with an increase in the speed of nozzle passage *s*.

[DOI: 10.22068/ijmse.4073]

Results show that the roughness *Ra* on average decreases by 2.25 times with an increase in the nozzle speed from 400 to 2000 mm/min.

We determine the relative change in roughness as

$$\Delta_R = \frac{Ra(s_{\max}, d) - Ra(s_{\min}, d)}{Ra(s_{\max}, d)}. \quad (1)$$

In our case $s_{\min}$=400 and $s_{\max}$=2000 mm/min, then the calculations using Eq. (1) shows that the relative change in roughness does not depend on the spraying distance and its value on average is about of Δ_R=0.6.

We found that logarithms of the roughness *Ra* and the speed of nozzle passage *s* are coupled by linear equation while *d* takes the fixed value (see Fig. 2)

$$\ln(Ra) = B - p\ln(s), \quad (2)$$

where *B* and *p* are empirical coefficients, which are calculated by least square method (see Table 3).

Therefore, the roughness of the coating surface depends on the speed of the nozzle passage as

$$Ra(s) = b \cdot s^{-p}, \quad (3)$$

where $r=e^B$ is the conditional roughness corresponding to the nozzle speed of one mm/min $r=Ra(s=1)$.

Calculations show that the values of R^2 are varies in the range of 0.84-0.99. Therefore, equation (3) adequately describes the experimental data observed. Thus, we propose the model sufficiently describing the dependence of the surface roughness of the coatings obtained by detonation spraying on the nozzle speed.

The results showed that varying the spray distance also affects the coating smoothness at a fixed detonation nozzle travel speed, except for the lowest speed (Table 2). It is obvious that at low speed of movement of the detonation nozzle, uniform spraying occurs regardless of the choice of spraying distance. When choosing faster speeds of movement of the nozzle from 800 mm/min, an extreme dependence of roughness on the spraying distance is observed. The surface relief of the coatings obtained at small spraying distances is characterized by high smoothness (low roughness). When choosing higher spraying distances, the roughness increases. The maximum roughness of the coating surface is achieved at spraying distances of 50-60 mm. Then the roughness decreases with further increase of spraying distance.

We found that the roughness *Ra* and spray distance *d* are coupled by parabolic equation while *s* takes the fixed value (see Fig. 3)

$$Ra(d) = a_2 d^2 + a_1 d + Ra_0, \quad (4)$$

[DOI: 10.22068/ijmse.4073]

where Ra_0 is the conditional roughness corresponding to the zero spray distance, $Ra_0=Ra(d=0)$; $a_{1,2}$ are the empirical coefficients, which are calculated by least square method (see Table 3).

Calculations show that the values of R^2 of the parabolic equation (4) are varied in the range of 0.73-0.96. Therefore, equation (4) adequately describes the experimental data observed. Thus, we propose the model sufficiently describing the dependence of the surface roughness of the coatings obtained by detonation spraying on the spray distance.

Obtained equation (4) allow us determining the maximal roughness value

$$Ra_m = Ra_0 - a_1^2 / 4a_2, \tag{5}$$

which can be obtained at the spray distance

$$d_m = -a_1 / 2a_2. \tag{6}$$

The obtained equations (5) and (6) can be used to select such a spraying distance of coatings at which the roughness of the surface will be the greatest. Such estimates can be useful in the production of self-cleaning coatings with the required wetting characteristics.

The parabolic equation (4) can be obtained within the framework of the phenomenological model under the assumption that the acceleration of the change in the surface roughness Ra with an increase in the spraying distance is constant:

$$Ra''(d) = 2a_2. \tag{7}$$

It is also assumed that the rate of change of the surface roughness with increasing spraying distance at a conditionally zero spraying distance is constant one:

$$Ra'(d=0) = a_1. \tag{8}$$

Relations (7) and (8) allow us to determine the physical and technological meaning of the empirical parameters of the parabolic equation (4) as follows: $a_1 = Ra'(d=0)$ и $a_2 = Ra''(d)/2$.

If we add the above-formulated relation in the form of an initial condition to relations (4) and (8) as follows

$$Ra(d=0) = Ra_0, \tag{9}$$

then we formally obtain the Cauchy problem for the ordinary differential equation (4) with initial conditions (8) and (9). The solution to the Cauchy problem is determined by the parabolic equation (4). Thus, the proposed phenomenological model based on the Cauchy problem describes the dependence of the surface roughness on the spraying distance in the production of coatings.

3.2 Thickness

[DOI: 10.22068/ijmse.4073]

Results of optical metallographic microscopy show that the thickness of coatings depends strongly on the speed of nozzle passage. Figure 4 shows the transverse polished sections of the thinnest (Fig. 4 *a*) and the thickest (Fig. 4 *b*). It is evident that the coatings are represented by a lamellar-granular structure formed by sprayed spherical titanium powder. The titanium oxide phase is clearly visible around the powder particles. A high level of adhesion to the substrate is visible. The contact zone has no pronounced defects.

The thicknesses of all coatings obtained using all 25 detonation spraying regimes used by us vary in the range from 119.4 to 771.8 μm. The average thickness of all coatings is 335.6±89.8 μm.

Results show that selecting a higher speed of nozzle passage results in samples with a thinner coating thickness at all spray distances (see Fig. 5). Therefore, one can say that the coating thickness h monotonically reduces with an increase in the speed of nozzle passage s.

Results show that the coating thickness on average decreases by 4.9 times with an increase in the nozzle speed from 400 to 2000 mm/min.

We determine the relative change in coating thickness as

$$\Delta_h = \frac{h(s_{\max}, d) - h(s_{\min}, d)}{h(s_{\max}, d)}. \tag{10}$$

The calculations using Eq. (10) show that the relative change in coating thickness does not depend on the spraying distance and its value on average is about of Δ_h=0.8.

We found that logarithms of the coating thickness h and the speed of nozzle passage s are coupled by a linear equation while d takes the fixed value (see Fig. 5)

$$\ln(h) = A - q\ln(s), \tag{11}$$

where A and p are empirical coefficients, which are calculated by least square method (see Table 5).

Therefore, the coating thickness depends on the speed of the nozzle passage as

$$h(s) = H \cdot s^{-q}, \tag{12}$$

where $H=e^A$ is the conditional coating thickness corresponding to the nozzle speed of one mm/min $H=h(s=1)$.

Calculations show that the values of R^2 are varied in the range of 0.985-0.999. Therefore, equation (11) adequately describes the experimental data observed. Thus, we propose the model sufficiently describing the dependence of the coating thickness obtained on the nozzle speed.

Experimental data (see Table 1) indicate that the thickness of the sprayed coating is practically independent of the spraying distance. This is also evident from the results of

[DOI: 10.22068/ijmse.4073]

calculations of the coefficients of Eq. (12), which change slightly at different values of the spraying distance (see Table 5).

We find the strong correlation between the thickness and roughness of the coatings (see Fig. 6). We obtain the following linear equation $Ra = 0.029 + 10.13 \cdot h$ with R^2=0.914. The resulting equation indicates that thicker coatings are characterized by greater roughness of their surfaces.

3.3 Hydrophobicity

One of the important characteristics of self-cleaning coatings is their wetting characteristics, which determine their hydrophobicity/hydrophilicity. We use such a characteristic as the wetting angle to assess the hydrophobicity of the obtained coatings.

The measured contact angles of all coatings obtained using all 25 detonation spraying regimes used by us vary in the range from 72.6° to 122.11°. The average contact angle for all coatings is 99.6±6.6°. Consequently, titanium coatings obtained by detonation in all considered regimes are hydrophobic.

We found that the contact angle θ and spray distance d are coupled by a parabolic equation while s takes the fixed value (see Fig. 7)

$$\theta(d) = b_2 d^2 + b_1 d + \theta_0, \tag{13}$$

where θ_0 is the conditional contact angle corresponding to the zero spray distance: θ_0=θ(d=0); $b_{1,2}$ are the empirical coefficients, which are calculated by least square method (see Table 6).

Calculations show that the values of R^2 of the parabolic equation (13) vary in the range of 0.81-0.99. Therefore, equation (13) adequately describes the experimental data observed. Thus, we propose the model sufficiently describing the dependence of the contact angle of the coatings obtained by detonation spraying on the spray distance.

Obtained equation (13) allow us determining the maximal contact angle value

$$\theta_m = \theta_0 - b_1^2 / 4b_2, \tag{14}$$

which can be obtained at the spray distance

$$d_m = -b_1 / 2b_2. \tag{15}$$

We can rewrite Eq. (13) using the maximal contact angle value and the spray distance defined by Eqs. (14) and (14) respectively as follows

$$\theta(d) = b_2 (d - d_m)^2 + \theta_m. \tag{16}$$

[DOI: 10.22068/ijmse.4073]

The obtained equations (14) and (15) can be used to select such a spraying distance of coatings at which the hydrophobicity of the surface will be the greatest. Such estimates can be useful in obtaining self-cleaning coatings with the best hydrophobic characteristics.

The parabolic equation (13) can be obtained within the framework of the phenomenological model under the assumption that the acceleration of the change in the contact angle with an increase in the spraying distance is constant:

$$\theta''(d) = 2b_2. \tag{17}$$

It is also assumed that the rate of change of the contact angle with increasing spraying distance at a conditionally zero spraying distance is constant one:

$$\theta'(d = 0) = b_1. \tag{18}$$

Relations (17) and (18) allow us to determine the physical and technological meaning of the empirical parameters of the parabolic equation (13) as follows: $b_1 = \theta'(d = 0)$ и $b_2 = \theta''(d)/2$.

If we add the above-formulated relation in the form of an initial condition to relations (17) and (18) as follows

$$\theta(d = 0) = \theta_0, \tag{19}$$

then we formally obtain the Cauchy problem for the ordinary differential equation (17) with initial conditions (18) and (19). The solution to the Cauchy problem (17)-(19) is determined by the parabolic equation (13). Thus, the proposed phenomenological model based on the Cauchy problem describes the dependence of the contact wetting angle on the spraying distance in the production of coatings.

Note that Eq. (13) adequately describes the dependence of the contact angle on the spray distance under regimes with the nozzle speed at 400, 800 and 2000 mm/min. A significant deviation from the parabolic dependence is observed at small spraying distances and the nozzle speeds of 1200 and 1600 mm/min. However, the contact angle values differ slightly at a spraying distance of 60 mm at all nozzle speeds. It is also clear that for most values of the nozzle speed, the highest value of the edge angle is observed on samples obtained at spraying distances of 50-60 mm. Therefore, such spraying distances can be considered optimal from the point of view of obtaining coatings with stable hydrophobic properties.

3.4 Discussion

It should be noted that the empirical relationships formulated above are based on an analysis of experimentally obtained data and are not derived from the first principles of the physics of detonation spraying. Nevertheless, such an approach is justified in the early stages

[DOI: 10.22068/ijmse.4073]

of studying complex multiphase processes such as detonation spraying, where the interaction of powder particles with the shock wave, their aerodynamic braking, melting, collision with the substrate, and subsequent consolidation are accompanied by strong nonlinearity and the interrelationship of multiple factors. Under such conditions, a rigorous analytical model describing the influence of nozzle velocity or distance to the substrate on coating morphology and adhesion requires consideration of a wide range of physical mechanisms, from particle dynamics in the detonation wave to thermomechanical processes during impact compaction and crystallization. Currently, such models, although being developed, remain computationally expensive and often require simplifying assumptions, limiting their predictive power in practical settings. In our case, titanium powder sprayed onto a steel substrate exhibits a clear trend: as the nozzle speed increases, the coating roughness decreases, consistent with a shorter buildup time for the deposited material and, consequently, a reduction in the size of the forming structural elements. At the same time, the roughness dependence on the distance to the substrate exhibits a non-monotonic pattern. An increase is observed with increasing distance up to a certain limit, followed by a subsequent decrease, which is likely related to a balance between particle cooling in flight (resulting in reduced deformability upon impact) and a decrease in kinetic energy (reducing the degree of their flattening and adhesion). It is precisely this non-monotonic pattern that is naturally approximated by a parabolic function in the empirical modeling. Thus, despite the lack of a rigorous theoretical conclusion, the proposed dependencies have practical value: they allow one to predict and control key coating characteristics within the studied ranges of process parameters and also serve as a starting point for subsequent in-depth physical and mathematical modeling, taking into account the mechanisms of mass, momentum, and energy transfer in the detonation flow.

In addition, we note that this study focuses primarily on the influence of detonation spraying process parameters on the morphology and wettability of the resulting coatings, while the phase composition and possible oxidation of titanium powder during spraying are only indirectly considered. Nevertheless, it should be noted that the mechanisms of phase transformations and oxidation of titanium powder during detonation spraying have been previously studied in detail in our papers [29, 37] where X-ray diffractometry (XRD), X-ray diffraction analysis (EDS), and energy-dispersive X-ray diffraction (XRD) analysis were used to demonstrate that, under typical detonation spraying conditions, pure titanium undergoes significant oxidation, forming lamellar structures with varying stoichiometries ranging from Ti to TiO_2.

[DOI: 10.22068/ijmse.4073]

4. Conclusions

We described the surface properties of metal-ceramic coatings based on titanium dioxide depending on the spraying conditions. We found that such properties as surface roughness, surface thickness, and its hydrophobicity can be controlled in the production process by selecting certain values of the technological parameters of the spraying process.

Based on the experiments we conducted, it was possible to determine the optimal values of the technological parameters of detonation spraying, ensuring maximum hydrophobicity of the produced coatings.

We found that the roughness of the coating surface and the coating thickness depend on the speed of the nozzle passage in accordance with the inverse power law. We obtain that the roughness and the contact angle depend on spray distance in accordance with a parabolic law. We proposed new equations that can be useful for predicting the characteristics of the coating surface, as well as for determining the optimal mode of spraying the coating, ensuring its best hydrophobicity. We formulate the Cauchy problems based on the second-order differential equations, the exact analytical solutions to which correspond to the fitting equations calculated.

The results of our paper can be useful for optimizing the process of manufacturing self-cleaning titanium dioxide coatings by detonation spraying with specified surface characteristics necessary to ensure the required hydrophobic properties.

Acknowledgments

The study was carried out within the framework of the implementation of the state task of the Ministry of Science and Higher Education of the Russian Federation No. FZWN-2023-0006 using equipment of the Center of High Technologies of the Belgorod V. G. Shukhov State Technological University and Joint Research Center “Technologies and Materials” of the Belgorod National Research University.

Declarations

Funding and/or Conflicts of interests/Competing interests

The authors declare that they have no known competing financial interests or personal relationships that could have appeared to influence the work reported in this paper.

Data Availability

No data were generated or analyzed in the presented research.

Funding Declaration

There is no funding.

[DOI: 10.22068/ijmse.4073]

Ethical Approval

Not applicable.

References

1. D. Zang, X. Xun, Ceramics Coated Metallic Materials: Methods, Properties and Applications. In: Advanced Ceramic Materials (M. Mhadhbi ed., IntechOpen, 2021) (2020). https://doi.org/10.5772/intechopen.93814.

2. C. Senderowski, Synthesis, Properties and Applications of Intermetallics, Ceramic and Cermet Coatings. Materials (Basel), **15**(23), (2022) 8408. https://doi.org/10.3390/ma15238408.

3. P. Jiang, Y. Zhang, R. Hu, B. Shi, L. Zhang, Q. Huang, Y. Yang, P. Tang, C. Lin, Advanced surface engineering of titanium materials for biomedical applications: From static modification to dynamic responsive regulation, Bioactive Materials, **27**, (2023) 15-57. https://doi.org/10.1016/j.bioactmat.2023.03.006.

4. K. Gao, Y. Zhang, J. Yi, F. Dong, P. Chen, Overview of Surface Modification Techniques for Titanium Alloys in Modern Material Science: A Comprehensive Analysis. Coatings, **14**(1), (2024) 148. https://doi.org/10.3390/coatings14010148.

5. R. Keshavamurthy, Be. Naveena, V. Tambrallimath, K. Prabhakar, Optimization of Deposition Parameters in Plasma Spray Coatings. In: Modeling and Optimization in Manufacturing. (2021) 217-235. https://doi.org/10.1002/9783527825233.ch8.

6. V. P. Haridasan, A. Velayudham, R. Krishnamurthy, Response surface modeling and parameter optimization of detonation spraying with enhanced coating performance, Materials Today: Proceedings, **46**, (2021) 3474-3481. https://doi.org/10.1016/j.matpr.2020.11.867.

7. M. Dang, S. Singh, H. King, J. Navarro-Devia, H. Le, T. Pattison, R. Hocking, S. Wade, G. Stephens, A. Papageorgiou, A. Manzano, J. Wang, Surface Enhancement of Titanium-Based Coatings on Commercial Hard Steel Cutting Tools. Crystals, **14**, (2024) 470. https://doi.org/10.3390/cryst14050470.

8. T. Xue, S. Attarilar, S. Liu, J. Liu, X. Song, L. Li, B. Zhao, Y. Tang, Surface Modification Techniques of Titanium and its Alloys to Functionally Optimize Their Biomedical Properties: Thematic Review. Front Bioeng Biotechnol. **8**, (2020) 603072. https://doi.org/10.3389/fbioe.2020.603072.

9. A. Kurup, P. Dhatrak, N. Khasnis, Surface modification techniques of titanium and titanium alloys for biomedical dental applications: A review, Materials Today: Proceedings, **39**, (2021) 84-90. https://doi.org/10.1016/j.matpr.2020.06.163.

10. N. Cherenda, A. Leyvi, A. Petuh, V. Uglov, S. Grigoriev, A. Vereschaka, V. Astashynski, A. Kuzmitski, Modification of Ti-6Al-4V titanium alloy surface relief by compression plasma flows impact. High Temperature Material Processes An International Quarterly of High-Technology Plasma Processes. **28**, (2024) 7-24. https://doi.org/10.1615/HighTempMatProc.2023050354.

11. V. Bhamare, R. Kulkarni, Methods for fabrication of ceramic coatings. In book: Advanced Flexible Ceramics. (2023) 215-242. https://doi.org/10.1016/B978-0-323-98824-7.00010-5.

12. M. Winnicki, Advanced Functional Metal-Ceramic and Ceramic Coatings Deposited by Low-Pressure Cold Spraying: A Review. Coatings, **11**(9), (2021) 1044. https://doi.org/10.3390/coatings11091044.

13. L. Singh, V. Chawla, J. Grewal, A Review on Detonation Gun Sprayed Coatings. Journal of Minerals and Materials Characterization and Engineering, 11(3), (2012) 243-265. https://doi.org/10.4236/jmmce.2012.113019.

14. Y. Tyurin, O. Kolisnichenko, J. Jia, N. Vasilik, M. Kovaleva, M. Prozorova, M. Arseenko, V. Sirota, Performance and Economic Characteristics of Multi-Chamber Detonation Sprayer Used in Thermal Spray Technology. Thermal Spray. Conference proceedings, (2016) 630-634. https://doi.org/10.31399/asm.cp.itsc2016p0630.

15. V. Y. Ulianitsky, D. K. Rybin, A. Sova, A. O. Moghaddam, M. Samodurova, M. Doubenskaia, E. Trofimov, Formation of metal composites by detonation spray of powder mixtures. Int. J. Adv. Manuf. Technol. **117**, (2021) 81-95. https://doi.org/10.1007/s00170-021-07743-7T.

16. D. V. Dudina, S. B. Zlobin, N. V. Bulina, A. L. Bychkov, V. N. Korolyuk, V. Yu. Ulianitsky, O. I. Lomovsky, Detonation spraying of TiO_2-2.5vol.% Ag powders in a reducing atmosphere, Journal of the European Ceramic Society, **32**(4), (2012) 815-821. https://doi.org/10.1016/j.jeurceramsoc.2011.10.022.

17. V. Yu. Ulianitsky, D.V. Dudina, I. S. Batraev, A. I. Kovalenko, N. V. Bulina, B. B. Bokhonov, Detonation spraying of titanium and formation of coatings with spraying atmosphere-dependent phase composition, Surface and Coatings Technology, **261**, (2015) 174-180 https://doi.org/10.1016/j.surfcoat.2014.11.038.

18. R. Sreekumar, R. V. Rao, Experimental Investigation and Parameter Optimization of Al_2O_3-40% TiO_2 Atmospheric Plasma Spray Coating on SS316 Steel Substrate, Materials Today: Proceedings, **5**(2), (2018) 5012-5020. https://doi.org/10.1016/j.matpr.2017.12.079.

19. N. Kumar, V. K. Choubey, Comparative Evaluation of Oxidation Resistance of Detonation Gun-Sprayed Al_2O_3-40%TiO_2 Coating on Nickel-Based Superalloys at 800°C

[DOI: 10.22068/ijmse.4073]

and 900°C. High Temperature Corrosion of mater, **99**, (2023) 359-373. https://doi.org/10.1007/s11085-023-10157-3.

20. M. Iesalnieks, R. Eglitis, T. Juhna, K. Šmits, A. Šutka, Photocatalytic Activity of TiO_2 Coatings Obtained at Room Temperature on a Polymethyl Methacrylate Substrate. Int. J. Mol. Sci. **23**, (2022) 12936. https://doi.org/10.3390/ijms232112936.

21. J. D. Bersch, I. Flores-Colen, A. B. Masuero, D. C. C. Dal Molin, Photocatalytic TiO_2-Based Coatings for Mortars on Facades: A Review of Efficiency, Durability, and Sustainability. Buildings, **13**, (2023) 186. https://doi.org/10.3390/buildings13010186.

22. J. Kasanen, M. Suvanto, T. Pakkanen, Self-cleaning, titanium dioxide based, multilayer coating fabricated on polymer and glass surfaces. Journal of Applied Polymer Science, **111**, (2009) 2597-2606. https://doi.org/10.1002/app.29295.

23. N. T. Padmanabhan, H. John, Titanium dioxide based self-cleaning smart surfaces: A short review. Journal of Environmental Chemical Engineering, **8**(5), (2020) 104211. https://doi.org/10.1016/j.jece.2020.104211.

24. N. V. Bulina, D. K. Rybin, S. V. Makarova, D. V. Dudina, I. S. Batraev, A. V. Utkin, I. Y. Prosanov, M. V. Khvostov, V. Y. Ulianitsky. Detonation Spraying of Hydroxyapatite on a Titanium Alloy Implant. Materials (Basel), **14**(17), (2021) 4852. https://doi.org/10.3390/ma14174852.

25. B. Rakhadilov, D. Baizhan, Creation of Bioceramic Coatings on the Surface of Ti–6Al–4V Alloy by Plasma Electrolytic Oxidation Followed by Gas Detonation Spraying. Coatings, **11**(12), (2021) 1433. https://doi.org/10.3390/coatings11121433.

26. S. M. Forghani, M. J. Ghazali, A. Muchtar, A. R. Daud, N. H. N. Yusoff, C. H. Azhari, Effects of plasma spray parameters on TiO_2-coated mild steel using design of experiment (DoE) approach, Ceram. Int., **39**(3), (2013) 3121-3127. https://doi.org/10.1016/j.ceramint.2012.09.092.

27. Lu Xie, Yue-Ming Wang, Xiang Xiong, Zhao-Ke Chen, Ya-Lei Wang, Effects of Oxygen Fuel Rate on Microstructure and Wear Properties of Detonation Sprayed Iron-Based Amorphous Coatings, Materials Transactions, **59**(12), (2018) 1867-1871.

28. V. Y. Ulianitsky, D. V. Dudina, A. A. Shtertser, I. Smurov Computer-Controlled Detonation Spraying: Flexible Control of the Coating Chemistry and Microstructure. Metals, **9**(12), (2019) 1244. https://doi.org/10.3390/met9121244.

29. V. V. Sirota, V .S. Vashchilin, Y. N. Ogurtsova, E. N. Gubareva, D. S. Podgornyi, M. G. Kovaleva, Structure and photocatalytic properties of the composite coating fabricated by detonation sprayed Ti powders. Ceramics International, **50**(1), (2024) 739-749. https://doi.org/10.1016/j.ceramint.2023.10.152.

[DOI: 10.22068/ijmse.4073]

30. V. V. Sirota, S. E. Savotchenko, V. V. Strokova, V. S. Vashchilin, D. S. Podgornyi, M. V. Limarenko, M. G. Kovaleva, Effect of irradiation intensity on the rate of photocatalysis of TiO2 coatings obtained by detonation spraying. International Journal of Applied Ceramic Technology, **21**, (2024). https://doi.org/10.1111/ijac.14782.

31. V. V. Sirota, S. E. Savotchenko, V. V. Strokova, V. S. Vashchilin, D. S. Podgornyi, D. S. Prokhorenkov, S. V. Zaitsev, M. G. Kovaleva, Effect of detonation spray regimes on photocatalytic activity of Ti-TiO2 coatings. Journal of Photochemistry & Photobiology, A: Chemistry, **452**, (2024) 115626. https://doi.org/10.1016/j.jphotochem.2024.115626.

32. B. Rakhadilov, D. Buitkenov, Z. Sagdoldina, B. Seitov, S. Kurbanbekov, M. Adilkanova, Structural Features and Tribological Properties of Detonation Gun Sprayed Ti–Si–C Coating. Coatings, **11**(2), (2021) 141. https://doi.org/10.3390/coatings11020141.

33. D. Buitkenov, B. Rakhadilov, B.T. Bauyrzhan, Z. Sagdoldina, A. Kenesbekov, Structure and Properties of Detonation Coatings Based on Titanium Carbosilicide. Key Engineering Materials, **821**, (2019) 301-306. https://doi.org/10.4028/www.scientific.net/KEM.821.301.

34. M. Kovaleva, Y. Tyurin, N. Vasilik, O. Kolisnichenko, M. Prozorova, M. Arseenko, V. Sirota, I. Pavlenko Structure and microhardness of titanium-based coatings formed by multichamber detonation sprayer. Physics Research International, **2015**, (2015) 532825. https://doi.org/10.1155/2015/532825.

35. M. G. Kovaleva, M. S. Prozorova, M. Yu. Arseenko, O. N. Vagina, V. V. Sirota Properties of Alumina-Titania Coating Formed by a New Multi-Chamber Gas-Dynamic Accelerator. Key Engineering Materials, **753**, (2017) 117-122. https://doi.org/10.4028/www.scientific.net/KEM.753.117.

36. V. Sirota, V. Pavlenko, N. Cherkashina, M. Kovaleva, Y. Tyurin, O. Kolisnichenko, Preparation of aluminum oxide coating on carbon/carbon composites using a new detonation sprayer, Int. J. Appl. Ceram. **2**, (2021) 483-489. https://doi.org/10.1111/ijac.1367.

37. V. V. Sirota, S. E. Savotchenko, V. V. Strokova, D. O. Bondarenko, D. S. Podgorny. Influence of the technological conditions of detonation coatings application on their phase composition. Nanotechnologies in construction, **16**(5), (2024) 404-414. https://doi.org/10.15828/2075-8545-2024-16-5-404-414.

[DOI: 10.22068/ijmse.4073]

Captions to the figures

Fig. 1. Optical images of the coating surfaces in the visible field (3000x2000 μm) applied under the constant spray distance (40 mm) and different speed of the nozzle passage 400 mm/min (*a*), and 2000 mm/min (*b*).

Fig. 2. Dependencies of the roughness *Ra* on the speed of the nozzle passage *s* (markers – experimental data from Table 1, solid lines – linear Eq. (2) with the values of coefficients from Table 3).

Fig. 3. Dependencies of the roughness *Ra* on the spray distance *d* (markers – experimental data from Table 1, solid lines – parabolic Eq. (4) with the values of coefficients from Table 4).

Fig. 4. Optical microscopy images of cross-sections of coatings applied under the constant spray distance (40 mm) and different speed of the nozzle passage 400 mm/min (*a*), and 2000 mm/min (*b*).

Fig. 5. Dependencies of the coating thickness *h* on the speed of the nozzle passage *s* (markers – experimental data from Table 1, solid lines – linear Eq. (11) with the values of coefficients from Table 5).

Fig. 6. Correlation plot of the roughness *Ra* and the coating thickness *h* (markers – experimental data from Table 1, solid line – linear equation: $Ra = 0.029 + 10.13 \cdot h$, R^2=0.914).

Fig. 7. Dependencies of the contact angle θ on the spray distance *d* (markers present the experimental data from Table 1, solid lines present the parabolic Eq. (13) with the values of coefficients from Table 6).

[DOI: 10.22068/ijmse.4073]

Figures

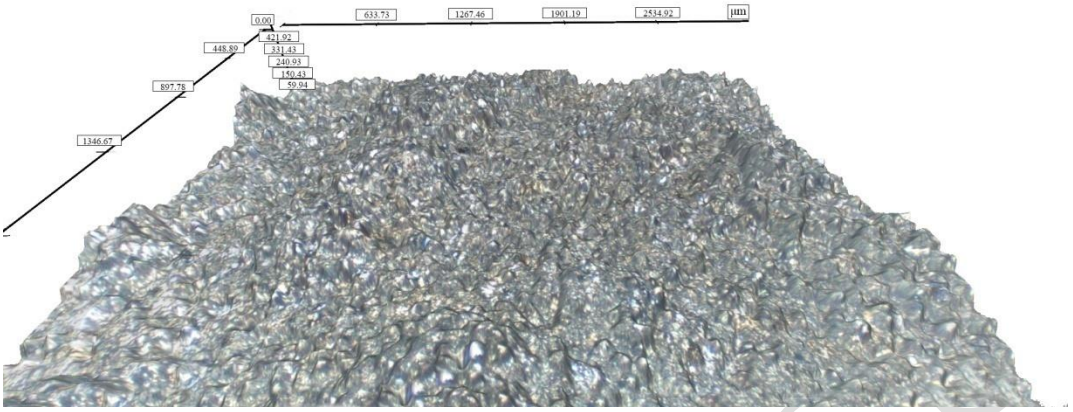

Fig. 1. *a*

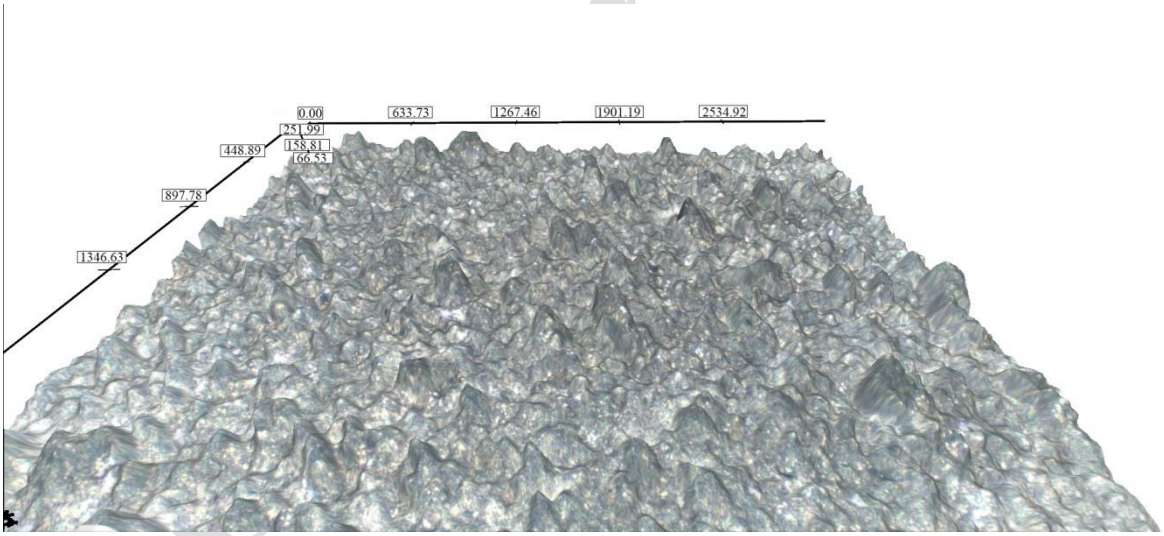

Fig. 1. *b*

[DOI: 10.22068/ijmse.4073]

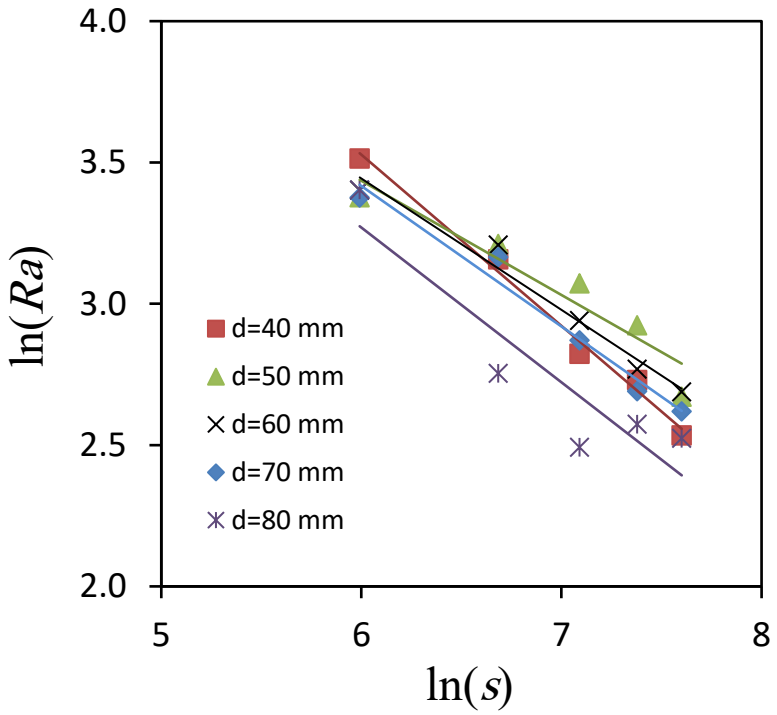

Fig. 2.

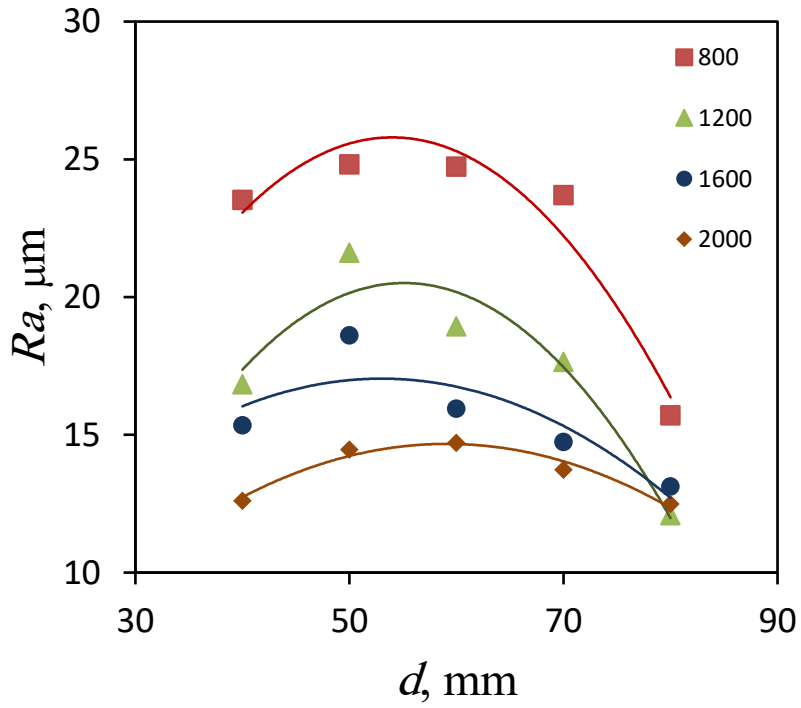

Fig. 3

[DOI: 10.22068/ijmse.4073]

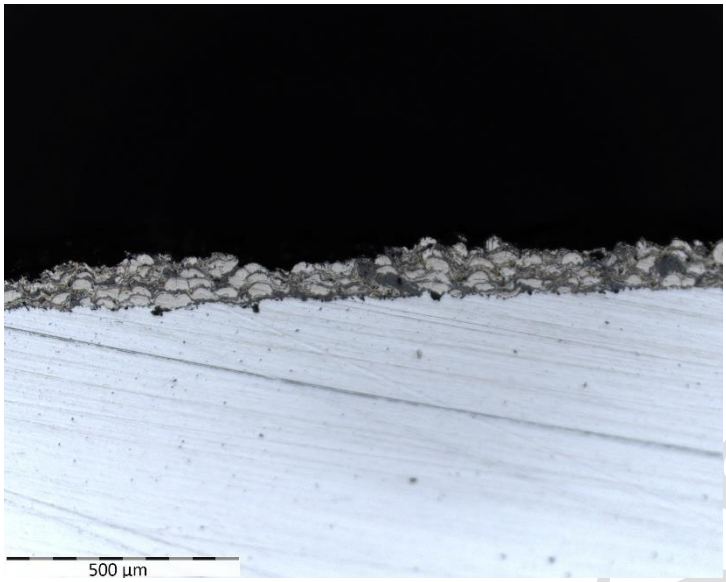

Fig. 4. *a*

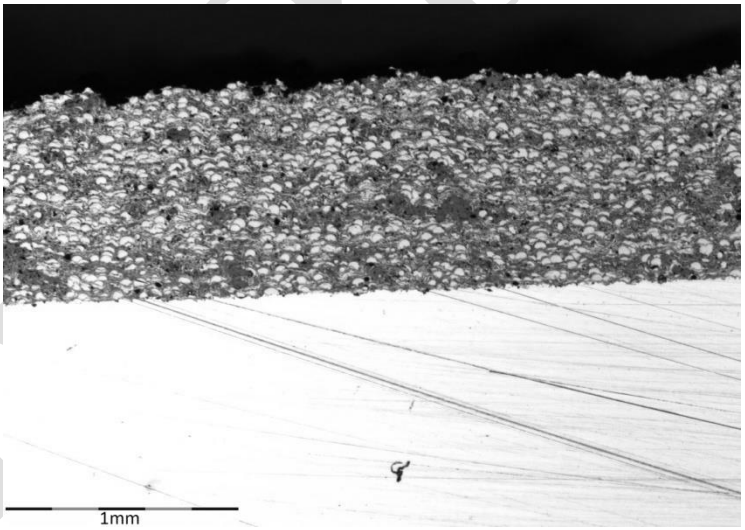

Fig. 4. *b*

[DOI: 10.22068/ijmse.4073]

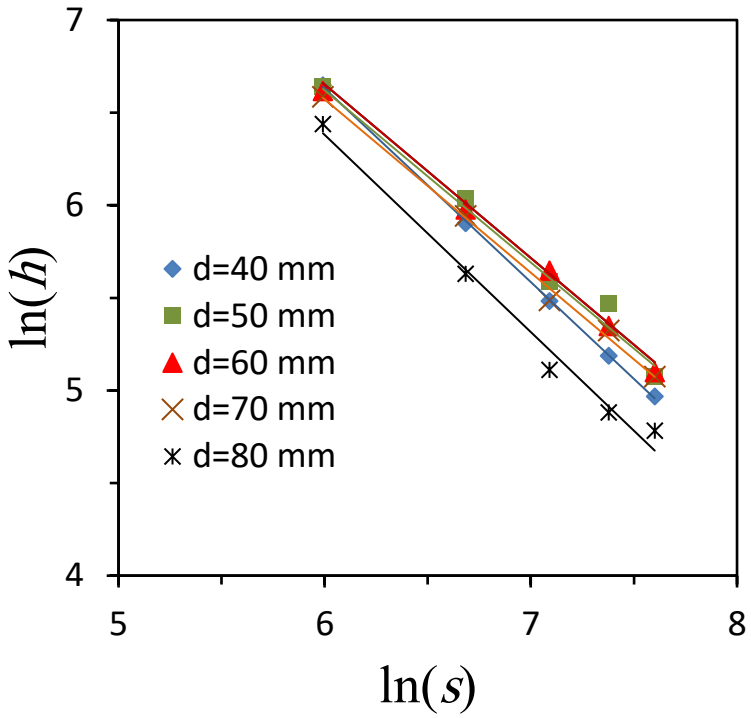

Fig. 5

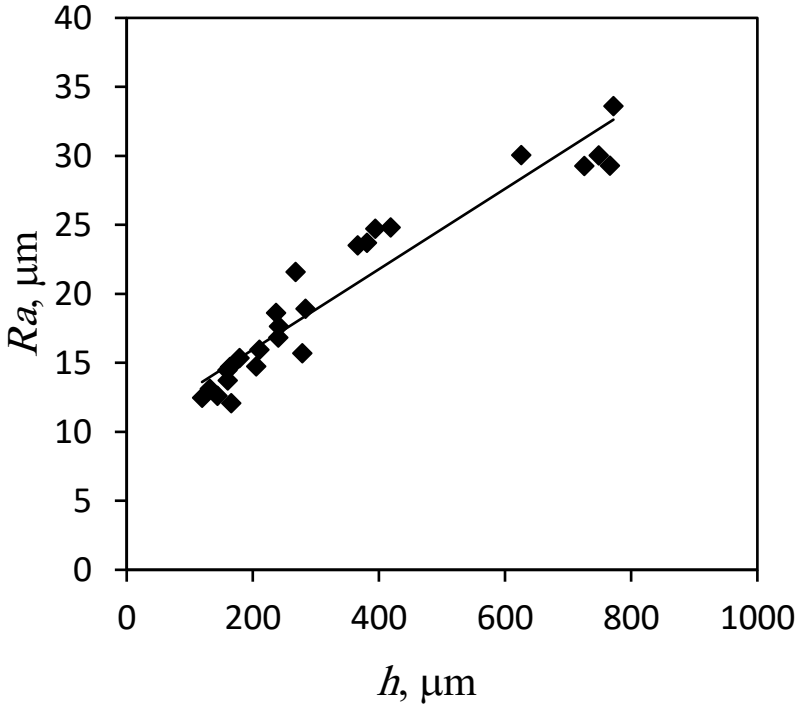

Fig. 6

[DOI: 10.22068/ijmse.4073]

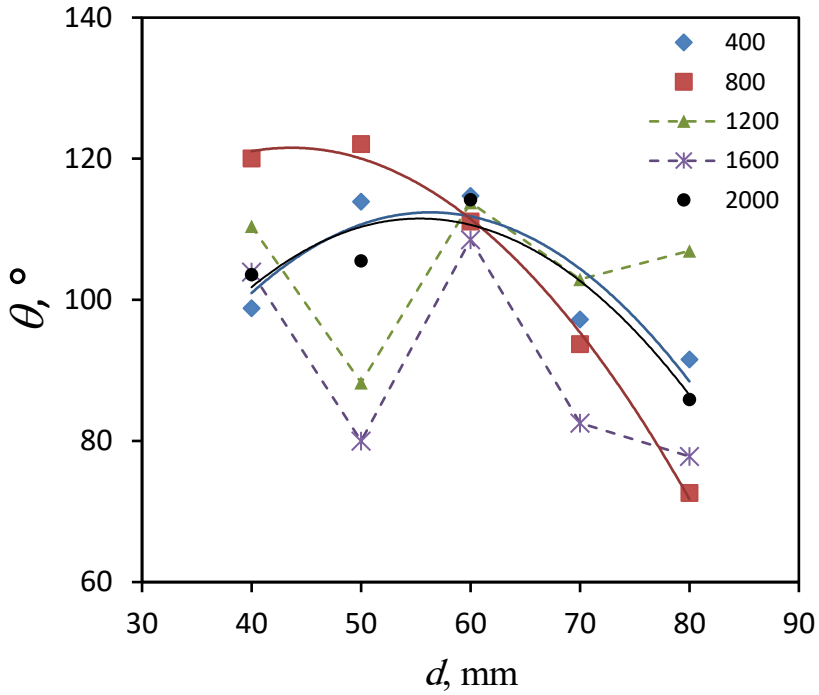

Fig. 7

[DOI: 10.22068/ijmse.4073]

Tables

Table 1. The thickness h and contact angle θ of the coatings obtained under different regimes with corresponding standard deviations σ_h, and σ_θ.

Regime number	d, mm	s, mm/mim	h, μm	σ_h, μm	θ,°	σ_θ,°
1		400	771.8	204.69	98.83	11.00
2		800	366.3	74.41	120.07	24.17
3	40	1200	240.6	46.97	110.44	37.15
4		1600	179.1	36.00	103.94	33.44
5		2000	143.9	28.97	103.60	32.52
6		400	766.4	138.56	113.95	10.61
7		800	418.8	75.31	122.11	10.18
8	50	1200	268.1	48.67	88.27	15.81
9		1600	237.1	49.98	77.00	14.18
10		2000	160.0	36.69	105.53	36.96
11		400	748.4	94.94	114.76	9.38
12		800	394.4	66.14	111.14	37.33
13	60	1200	283.8	30.82	113.79	15.61
14		1600	210.4	35.78	108.55	46.69
15		2000	163.9	33.18	114.23	24.79
16		400	725.8	182.21	97.22	23.89
17		800	381.1	62.02	93.74	32.06
18	70	1200	241.7	40.01	102.89	20.85
19		1600	205.2	48.50	82.52	31.91
20		2000	160.1	26.84	72.55	18.77
21		400	625.8	91.44	91.55	27.79
22		800	278.7	42.22	72.66	25.84
23	80	1200	166.1	25.42	106.94	12.26
24		1600	132.0	29.99	77.81	30.70
25		2000	119.4	28.60	85.92	15.07

[DOI: 10.22068/ijmse.4073]

Table 2. Surface roughness of the coatings obtained under different regimes with corresponding standard deviations σ_{Ra}, σ_{Rz}, and σ_{Rmax}

Regime number	*Ra*, μm	σ_{Ra}, μm	*Rz*, μm	σ_{Rz}, μm	*Rmax*, μm	σ_{Rmax}, μm
1	33.62	17.91	169.63	95.83	170.49	73.78
2	23.53	12.55	119.95	64.52	95.74	59.36
3	16.84	7.97	95.83	44.25	95.15	35.33
4	15.35	6.93	98.21	57.88	99.29	40.15
5	12.61	4.47	78.69	40.43	78.74	29.88
6	29.29	15.75	145.32	84.35	145.17	69.88
7	24.82	12.03	129.62	66.74	131.75	56.13
8	21.61	10.26	128.49	62.72	127.61	47.47
9	18.62	7.36	112.71	59.07	113.69	41.14
10	14.47	6.22	88.58	44.90	87.75	34.40
11	30.05	16.51	151.42	85.54	150.99	69.37
12	24.74	11.37	131.42	66.82	131.83	49.11
13	18.94	8.97	106.02	52.61	105.54	45.32
14	17.97	9.10	103.23	55.74	102.47	41.24
15	14.71	5.90	89.02	43.98	89.37	40.86
16	29.28	15.34	145.00	81.18	143.71	66.87
17	23.71	9.92	122.35	64.92	123.48	48.46
18	17.65	7.35	103.88	57.16	105.52	39.79
19	14.75	5.48	90.28	47.88	90.90	34.54
20	13.74	4.74	83.91	38.94	84.09	27.38
21	30.06	19.46	150.20	98.95	149.61	82.00
22	15.71	8.67	88.09	50.15	88.79	40.36
23	12.09	5.28	69.81	39.98	70.65	30.47
24	13.13	6.01	81.69	44.05	81.61	32.14
25	12.49	4.38	77.61	39.63	77.64	28.01

Table 3. The values of parameters of Eqs. (2) and (3) with different spray distances

d, mm	*r*	*B*	*p*	R^2
40	1289.79	7.162	0.605	0.989
50	350.72	5.860	0.404	0.903
60	508.77	6.232	0.464	0.971
70	600.64	6.398	0.497	0.971
80	702.75	6.555	0.547	0.843

[DOI: 10.22068/ijmse.4073]

Table 4. The values of parameters of Eq. (4) with different nozzle speed

s, mm/min	a_2	a_1	Ra_0	R^2
800	–0.013	1.506	–14.870	0.936
1200	–0.013	1.518	–21.320	0.917
1600	–0.005	0.629	0.362	0.734
2000	–0.005	0.627	–3.858	0.959

Table 5. The values of parameters of Eqs. (11) and (12) with different spray distances

d, mm	$H\times10^5$	A	q	R^2
40	4.003	12.90	1.045	0.999
50	2.132	12.27	0.936	0.986
60	1.949	12.18	0.935	0.995
70	1.968	12.19	0.929	0.997
80	3.480	12.76	1.064	0.985

Table 6. The values of parameters of Eq. (13) with different nozzle speed

s, mm/min	b_2	b_1	θ_0	R^2
400	–0.042	4.824	–23.50	0.806
800	–0.037	3.282	49.94	0.994
2000	–0.041	4.558	–14.67	0.906

[DOI: 10.22068/ijmse.4073]